Journal of Non-Crystalline Solids 357 (2011) 814–819

Contents lists available at ScienceDirect

Journal of Non-Crystalline Solids

journal homepage: www.elsevier.com/ locate/ jnoncrysol

A study of mechanical homogeneity in as-cast bulk metallic glass by nanoindentation

J.D. Plummer [a,*], R. Goodall [a], I.A. Figueroa [a,b], I. Todd [a]

[a] Department of Materials Science and Engineering, University of Sheffield, Mappin St., Sheffield S1 3JD, UK
[b] Instituto de Investigaciones en Materiales, UNAM, 04510 México D. F., Mexico

ARTICLE INFO

Article history:
Received 25 September 2010
Received in revised form 1 November 2010
Available online 29 November 2010

Keywords:
Metallic glass;
Nanoindentation;
Plasticity;
Fragility

ABSTRACT

A surface softening effect induced during copper-mould suction casting of bulk metallic glass is investigated as a function of rod diameter and glass fragility index, *m*, by nanoindentation. A reduction in hardness and reduced modulus at the rod surface is found to be favoured in small diameter castings and in fragile systems, respectively resulting from limited *in-situ* annealing and from a greater diversity of metastable atomic environments in the potential energy landscape of fragile glasses. Enhanced propensity for shear transformation zone nucleation in the low moduli surface is explained in terms of reduced atomic connectivity arising from a reduction in local co-ordination number and a lowering of the shear modulus. Finally, the structure and mechanical diversity that is possible in as-cast bulk metallic glass rods is explored through a relative quantification of shear modulus and plastic zone size across the whole as-cast state and in a single rod. These findings illustrate the sensitivity of bulk metallic glass to preparation, especially in respect of thermal history, potentially making replication of mechanical data between researchers problematic.

1. Introduction

The mechanism through which bulk metallic glasses (BMGs) yield involves the co-operative shearing of a local atomic environment, proposed to be of the order of 100 atoms, termed shear transformation zones (STZs) [1]. The shear modulus, *G*, is believed to provide the principal barrier to this event, although, based on models for shear in an amorphous granular material where a small dilatational strain is exerted on the surroundings, the bulk modulus, *B* also would be expected to provide a contribution to the activation energy [2]. A band of reduced viscosity subsequently propagates from the STZ, allowing for plastic deformation, before void formation occurs in the band [3], developing into a crack and causing failure. As plasticity is mediated by both the nucleation of a shear band at an STZ and its subsequent propagation, its attainment in BMGs requires that both these stages of plastic deformation are understood, and that they may be controlled.

A local reduction in atomic bond density creates a more fertile site for STZ nucleation. This is the principle central to the idea of Poon et al. [4] which suggests that brittle behaviour, indicated by a low Poisson's ratio, ν, can be alleviated by a low ratio of local shear modulus to global modulus, $G^*/\langle G\rangle$. Similarly, Cheng et al. [5] conceptually separated the elemental (G_e) and configurational (G_c) contribution to elastic moduli in BMGs, and believed that brittle alloy systems, such as those based on Fe, Mg, Ce etc., require significant local reductions in *G* to encourage multiple STZ nucleation. One might suggest that basing the prediction or explanation of plastic strain in BMGs on measured global elastic moduli, such as by sound wave measurement techniques, averages local perturbations in modulus, and so sensitivity to the dependence of mechanical behaviour on the ability for a local structure to co-operatively collapse is lost.

A soft surface layer has been reported for a 2 mm diameter rod of $Cu_{50}Zr_{50}$ in the as-cast condition [6]. Instrumented nanoindentation, performed along a traverse from the edge of the casting towards the centre, revealed a 13% drop in elastic modulus between the two ends of the line which was ascribed to the differing cooling conditions at the centre and edge during copper-mould casting of BMG rods generating more atomic defects at the surface as compared to the centre-line. The local moduli of this sample vary between the edge and centre of the rod, and so a quantification of these moduli by standard techniques will not provide sensitivity to the composite nature of the rod, with respect to atomic environments.

Nanoindentation allows the structural response of a material to be investigated in a controlled manner, typically without the risk of failure in the case of more brittle materials. It has been implemented to study the deformation characteristics and tendency for shear banding in BMGs [7,8] and enables the probing of a small region, where the generated shear stress ahead of the indenter is sufficient to induce shear banding, without influencing the surrounding bulk. This has led to the development of theory relating to shear band activity as a function of loading rate [7] and temperature [8], through an analysis of the extent of serrated flow, with the corresponding “pop-in” events (a rapid increase in depth with little or no increase in load) indicating the activation of a shear band. In this study we use nanoindentation to investigate and probe the extent of hardness and elastic modulus

* Corresponding author. Tel.: +44 114 222 5943.
E-mail address: j.plummer@sheffield.ac.uk (J.D. Plummer).

0022-3093/$ – see front matter © 2010 Elsevier B.V. All rights reserved.
doi:10.1016/j.jnoncrysol.2010.11.002

variation across as-cast and annealed BMG rods. This is performed as a function of section diameter and with BMG composition, characterised by the fragility index, m, which quantifies the rate of change of viscosity as the glass transition temperature, T_g, is approached.

2. Experimental

$Pd_{77.5}Si_{16.5}Cu_6$, $Zr_{65}Cu_{15}Al_{10}Ni_{10}$ and $Ce_{70}Al_{10}Cu_{10}Ni_{10}$ were selected for this study owing to their range of fragility index values (52, 30 and 21 respectively) and their differing propensities to demonstrate plastic flow; selected properties can be found in Table 1. 10 g ingots of each alloy were generated by arc melting high purity constituents (≥99.6%) in an environment evacuated to 5×10^{-3} Pa and then backfilled with 1/3 of an atmosphere of argon. A Ti "getter" was melted prior to sample melting to favour the creation of a localised high vacuum, and ingots were flipped and re-melted four times to ensure chemical homogeneity and complete melting. An *in-situ* copper-mould suction casting facility enabled the production of amorphous rods, all from the same ingot for a single alloy, with a range of diameters (1 mm–4 mm). Their glassy structure was analyzed by x-ray diffraction using CuKα radiation; thin slices were cut from the rod enabling the probing of the structure through the entire cross-section. Diameters up to the largest over which each BMG composition could be cast and remain fully amorphous, within the limits of determination by the x-ray diffraction technique, were used in this study; 3 mm for $Pd_{77.5}Si_{16.5}Cu_6$, 4 mm for $Zr_{65}Cu_{15}Al_{10}Ni_{10}$ and 1 mm for $Ce_{70}Al_{10}Cu_{10}Ni_{10}$. It would be anticipated that $Ce_{70}Al_{10}Cu_{10}Ni_{10}$ may display the largest glassy diameter, as it is, on the basis of measured fragility index, the strongest glass former. The inability to generate larger sections is considered to originate from sensitivity to impurities acting as heterogeneous nucleation agents; the large negative enthalpy of formation of Ce_2O_3 (−1823 kJ/mol [11]) will drive the reaction of Ce with dissolved oxygen, increasing the number density of nucleation sites, with these potentially acting to promote crystal formation and thereby reducing the glass forming ability of the alloy. Whilst the large negative enthalpy of formation of rare-earth oxides can act as oxygen scavengers when added in small amounts to base glass forming alloys, improving critical diameters [12], as $Ce_{70}Al_{10}Cu_{10}Ni_{10}$ is the glass forming composition it may exhibit strong sensitivity to impurities with respect to glass formation. After casting, BMG rods were sectioned on a slow speed precision diamond cut-off saw and cold mounted in resin parallel to the cut surface for subsequent grinding and polishing, giving a high quality mirrored finish. Samples of the largest diameter cast for each alloy were heat treated in a high vacuum furnace (5×10^{-4} Pa) for 5 hours at 0.6 of the glass transition temperature ($0.6T_g$).

Nanoindentation was performed on a Hysitron Nanomechanical Tester, fitted with a Berkovitch diamond tip, using an applied load of 6 mN with a load, hold and unload segment time of 5 s each, obtaining hardness, H_v, and reduced modulus, E_r, data. H_v is defined as the maximum applied load divided by the resulting indent area and E_r is computed from Eq. (1) [13], where, respectively, E and E_i are the elastic moduli of the sample and indenter, and ν and ν_i the Poisson's ratios of the sample and indenter.

$$\frac{1}{E_r} = \frac{\left(1-\nu^2\right)}{E} + \frac{\left(1-\nu_i^2\right)}{E_i} \tag{1}$$

Table 1
Selected properties for the alloys studied; elastic moduli (E, G and B), glass transition temperature, T_g, plastic strain, ε_p, and fragility index, m.

	E (GPa)	G (GPa)	B (GPa)	T_g (K)	ε_p (%)	m	Ref.
$Pd_{77.5}Si_{16.5}Cu_6$	88.8	31.5	167	635	10.4	52	2,9
$Zr_{65}Cu_{15}Al_{10}Ni_{10}$	83.0	30.3	106.7	653	0.12	30	2,9
$Ce_{70}Al_{10}Ni_{10}Cu_{10}$	30.3	11.5	27	359	0	21	2,10

E_r thus provides a measure of the elastic modulus, though it includes a contribution from the elastic properties of the indenter. H_v and E_r profiles were obtained for the cross-section of each diameter rod by performing indentation traverses from the edge of the rods to the centre at 10 μm steps for the first 450–500 μm and then in groups of four steps at 100 μm intervals. This method permits increased data acquisition in the region of interest (i.e. the rod surface). Three parallel traverse lines were used with a spacing of 10 μm between them to obtain an average H_v and E_r for each location, aiding reduced spread in the results.

3. Results

The unloading portion of indentation curves can be used to extract data pertaining to H_v and E_r [13]. For the samples tested here, the resulting reduced elastic modulus and hardness traverses can be seen in Figs. 1 and 2 respectively. Reducing sample diameter induces a reduction in H_v and E_r across the whole traverse, i.e. the statistical average of all measurements decreases as rod diameter decreases; this is considered, and hereafter called, a global softening effect, as it would be expected that it would be perceived as such in conventional mechanical tests on macroscopic specimens. Whilst pronounced surface softening can be seen in some of the traverses, it is not apparent in all; the magnitude of the effect decreases with increasing sample size, and subsequently disappears beyond a critical size.

In order to compare the relative magnitudes of the softening effect between the alloys, E_r is used in place of H_v. Work softening of BMGs [14] is anticipated to potentially influence H_v, the extent of which will be a function of the local structure and is thus not constant for each indentation. This may be the origin of increased scatter in H_v as compared to E_r (see Figs. 1 and 2). Data for the surface reduction in E_r is contained in Table 2 where, in an attempt to reduce the variation to a simple quantitative parameter, the edge result is divided by that obtained in the centre, enabling direct comparison without the relative magnitude of the values influencing the analysis. The Pd-based glass shows an almost identical effect in the 1 mm and 2 mm rods with a reduction of 13% and 12% respectively in E_r at the edge versus that of the centre-line. Although the Zr-based glass shows the largest drop-off of 23% for 1 mm diameter samples, this reduces to just 5% when the sample diameter increases to 2 mm. $Zr_{65}Cu_{15}Al_{10}Ni_{10}$ therefore has increased sensitivity to diameter with regard to the magnitude of the surface phenomenon. Lastly, the Ce-based alloy shows only a slight decrease in E_r of 6% at the surface, the lowest for all the 1 mm specimens. It can be seen that the more fragile Pd-based BMG can most favourably retain a surface reduction effect, whilst the ability to do this is much reduced for the least fragile Ce-based alloy.

Typical load/unload curves at varying locations and rod size can be seen in Fig. 3. The loading curves for the $Pd_{77.5}Si_{16.5}Cu_6$ and $Zr_{65}Cu_{15}Al_{10}Ni_{10}$ samples feature a number of pop-ins, indicating that shear systems have been activated. Serrated flow is more prevalent at the edge of the 1 mm rods than at the centre of both the 3 mm and 4 mm samples for $Pd_{77.5}Si_{16.5}Cu_6$ and $Zr_{65}Cu_{15}Al_{10}Ni_{10}$ respectively. Pop-in events are more restricted in the annealed samples of the Pd-based and Zr-based alloys and in as-cast and annealed $Ce_{70}Al_{10}Cu_{10}Ni_{10}$. Maximum indenter penetration depth is visible in $Pd_{77.5}Si_{16.5}Cu_6$ and $Zr_{65}Cu_{15}Al_{10}Ni_{10}$ specimens with the lowest diameter and, during the load hold, some creep-like phenomena are enhanced at the edge of the smallest samples for each alloy. Depth penetration is restricted in the annealed alloys. These results show a variation in hardness as a function of indenter location, rod size and whether or not they have received an annealing treatment; the smaller the diameter of the sample, and the closer to the surface, the softer the structure is and the more shear band activity is generated.

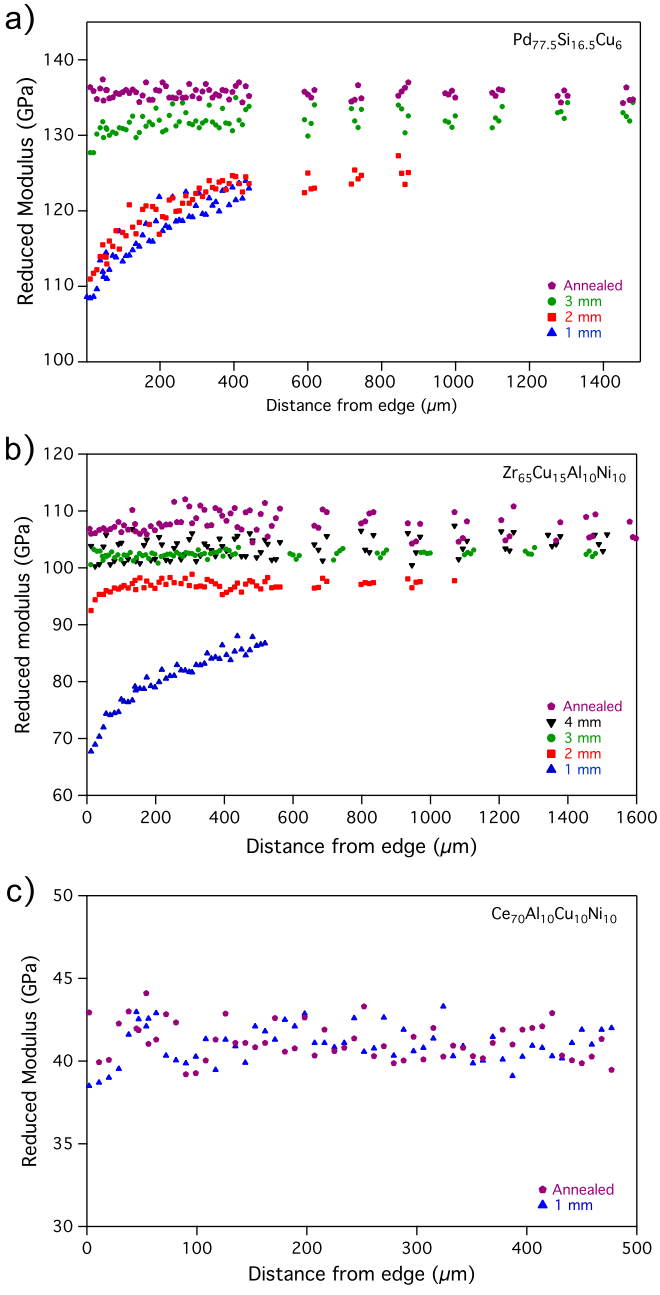

Fig. 1. Reduced modulus, E_r, profiles from the edge of as-cast BMG rods towards the centre for (a) $Pd_{77.5}Si_{16.5}Cu_6$, (b) $Zr_{65}Cu_{15}Al_{10}Ni_{10}$ and (c) $Ce_{70}Al_{10}Cu_{10}Ni_{10}$. Rod diameter indicated on graph.

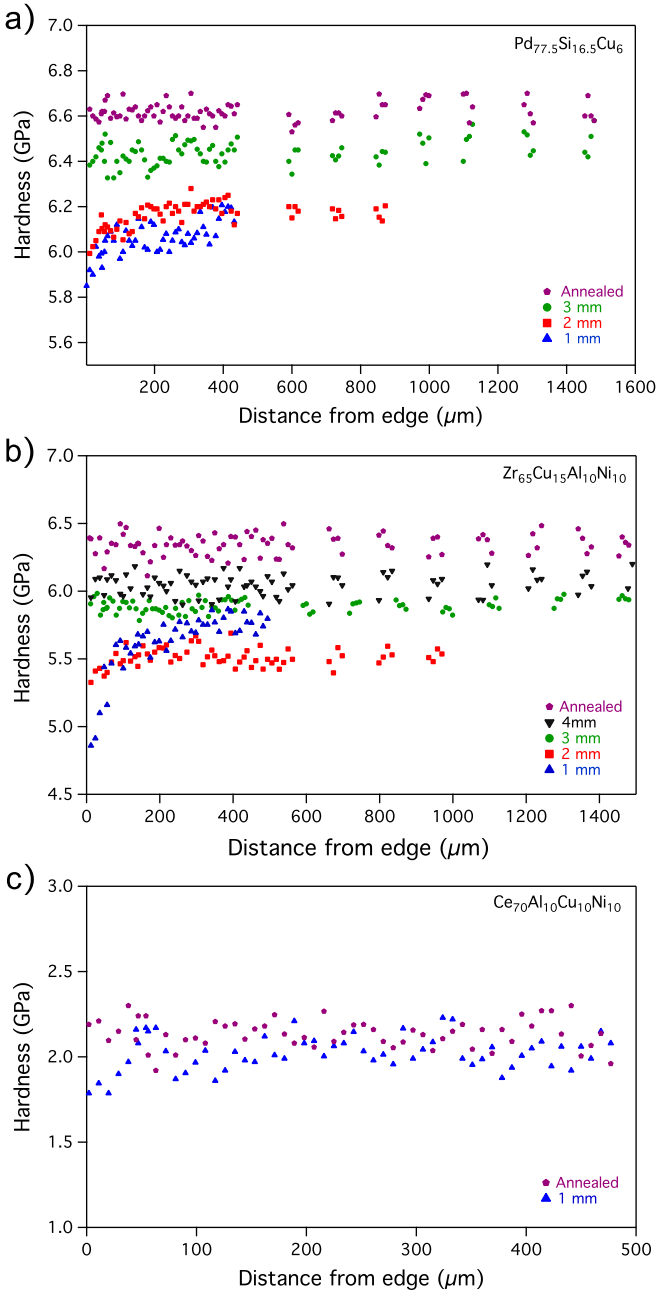

Fig. 2. Hardness, H_v, profiles from the edge of as-cast BMG rods towards the centre for (a) $Pd_{77.5}Si_{16.5}Cu_6$, (b) $Zr_{65}Cu_{15}Al_{10}Ni_{10}$ and (c) $Ce_{70}Al_{10}Cu_{10}Ni_{10}$. Rod diameter indicated on graph.

4. Discussion

Liu et al. derived an expression to relate defect concentration to cooling rate, where proportionality between the two was suggested [6]. As a result of the higher cooling rate at the surface of BMGs as compared to the centre, it was considered that surface softening of BMGs is universal and is thus present in all copper-mould suction cast rods. The data presented here suggests differently and that the extent of surface softening is dependent on two factors: 1) sample size, and 2) glass fragility index. With regard to sample size, the magnitude of the surface softening in the Pd- and Zr-based alloys is seen to decrease with increasing sample size, despite the cooling rate generally being higher at the surface of each casting. As the radial distance over which heat is extracted increases however, the surface will experience a slower cooling rate, allowing for more atomic movement and structural relaxation. A greater *in-situ* annealing effect also takes place in larger diameter samples, where the surface is held at elevated temperatures, which is sufficient for atomic relaxation, for longer time periods. This results in the magnitude of surface softening decreasing in the Pd- and Zr-based glasses as sample diameter is increased.

The concept of a potential energy landscape (PEL) defines a multi dimensional surface, where the energy of available structural states (defined with regard to position, orientation and vibration co-ordinates) is given, and minima in the energy landscape are thus representative of different atomic co-ordinations, or inherent states (IS). The crystalline state can be considered the lowest energy configuration minima (or basin) in a PEL, with glassy states having minima in energy very close to the crystalline potential. PELs of strong

Table 2
Comparison of relative surface drop-off in reduced modulus, E_r.

	Rod diameter (mm)	$\frac{E_{r(edge)}}{E_{r(centre)}}$
$Pd_{77.5}Si_{16.5}Cu_6$	1	0.87
	2	0.88
	3	0.96
$Zr_{65}Cu_{15}Al_{10}Ni_{10}$	1	0.77
	2	0.95
	3	1.00
	4	1.00
$Ce_{70}Al_{10}Ni_{10}Cu_{10}$	1	0.94

glass formers contain less "features" corresponding to a reduced number of local environments that can be sampled in a glassy structure [15–17]. This is illustrated schematically in Fig. 4. A wide range of local minima exist in the PEL of a high m (fragile) glass however. To illustrate this point, amorphous silica follows a near Arrhenius viscosity temperature dependence, indicating almost constant activation energy across the temperature range for viscous flow [17], and it is this that distinguishes it as a strong glass former, as compared to a fragile system where the activation energy rapidly increases as T_g is approached. This implies that the atomic movements that are required for flow are the same at all temperatures in amorphous silica, and so the energy landscape can be expected to consist of minima of approximately equal depth. When a strong glass forming BMG is cast, the lack of different IS means the structure at the surface is more similar to that in the centre. Therefore, despite the surface experiencing a higher cooling rate, a limited number of IS are permitted and so the structure has to conform to similar configurations to those in the rod centre. Fragile glasses however have a number of features in their PEL, and so a greater range of metastable atomic configurations. Thus, when the surface is rapidly cooled it stabilises into different energy minima than in the slower cooled centre. It may be that fragile glasses are most effective at exhibiting surface softening.

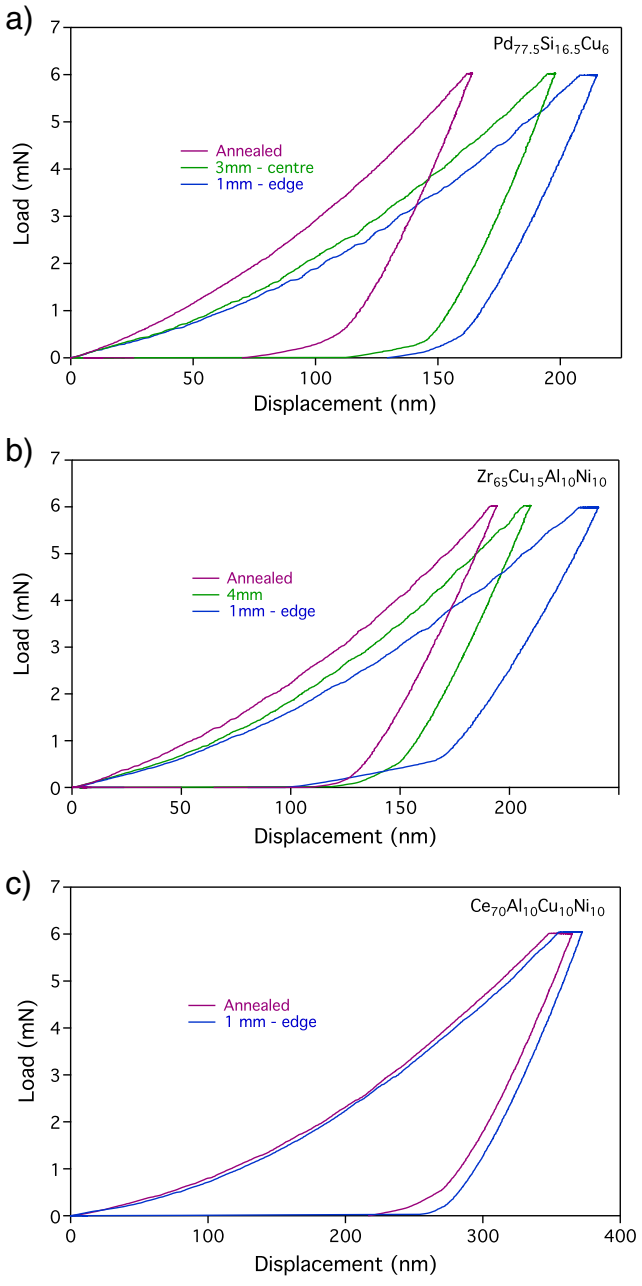

Fig. 3. Load/unload curves for (a) $Pd_{77.5}Si_{16.5}Cu_6$, (b) $Zr_{65}Cu_{15}Al_{10}Ni_{10}$ and (c) $Ce_{70}Al_{10}Cu_{10}Ni_{10}$. Rod diameter indicated on graph.

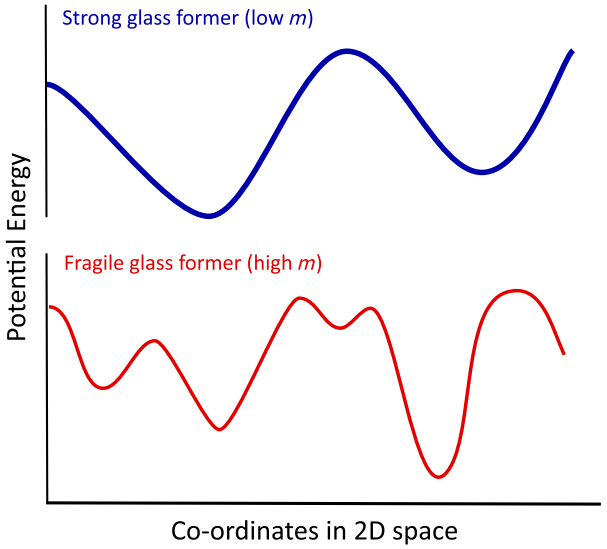

Fig. 4. Schematic illustration of the potential energy landscape of strong and fragile glass forming systems.

The observation of increased pop-in phenomena in Fig. 3 occurs in the lowest H_v and E_r structural states i.e. at the edge of the samples that surface soften as compared to the annealed states, where more structural relaxation has occurred. Since all samples tested for any given alloy were from the same ingot, compositional variation is not the source of the different mechanical response, and so it is the structural aspect that is dominating behaviour. Since the activation energy of a shear event in a glassy substance, be it thermal or mechanical, is dependent on G, the enhanced tendency to shear banding originates from a reduction in elastic moduli. This may be explained by invoking arguments regarding the extent of local atomic connectivity. Atomic rearrangement requires that bond breaking and subsequent re-formation occur; the local co-ordination number will have an influence on this as it will dictate the number of bonds that must be broken. Minima in PELs correspond to stable co-ordination numbers, with higher energy states representing less favourable environments that contribute more elastic energy to a shear process [18]. Rapid surface cooling freezes the structure into these less stable states [17] (with increased propensity in fragile systems as previously mentioned) resulting in an improved tendency for shear banding at these locations, realised as a transfer between minima in the energy landscape. Our future work will consider local co-ordination in

different regions of surface softened rods so to further characterise the structural and mechanical differences discussed here.

A measure of G for the data in Fig. 1 would permit an understanding of the activation barrier to STZ nucleation, and to subsequent plastic strain. This will only be a function of structural state as it is a reasonable assumption that the chemical contribution is unaffected by indentation location, i.e. the cast rods are chemically homogeneous. Plotting G versus E (Fig. 5), for the range of BMGs and oxide glasses in Table 1 of both [1] and [19], yields a strong linear relationship allowing G to be estimated directly from E in BMGs, irrespective of their differing ν; a simple linear least squares regression gives $G = 0.38E$. This value of proportionality between G and E is in accordance with that of 0.39, which has previously been found in polycrystalline metals [20]. For the E_r data determined in this study, difficulties exist in calculating the absolute E using Eq. (1) as ν varies with thermal history, and so will differ with location in the samples. However, using Fig. 5 some measure of the shear modulus, G^*, can be determined from E_r. This value is not comparable with G due to the elastic contribution from the indenter and the fact that the local ν at each location cannot be determined. However, it does permit a measure of the configurational G to be deduced, due to the elemental contribution being constant for each location, based on the assumption of chemical homogeneity. Then, G^* within a 1 mm rod and across the whole as-cast state for an alloy are representative of changes in G. The range can be characterised by dividing the maximum value by the minimum, to give a value illustrative of the structural variation in G:

$$\left(\frac{G^*_{edge}}{G^*_{centre}}\right)_{1mm} \tag{2}$$

$$\left(\frac{G^*_{min}}{G^*_{max}}\right) \tag{3}$$

The values in Table 3 demonstrate the differences in G^* that are encountered within cast BMG rods, due to surface and global softening and represent significant differences in G^* as a function of the cast state. Rather than using the annealed samples for G^*_{max}, the centre of the largest diameter as-cast sample is taken to highlight the magnitude of the difference in G across as-cast states instead of in those that have undergone secondary processing. As an example, $Pd_{77.5}Si_{16.5}Cu_6$ shows a 13% difference between the centre and edge of a 1 mm rod and a 40% difference between the edge of the 1 mm rod and the centre of the 3 mm sample. This range of G values helps to explain why shear bands are less activated when the structural state tends towards being fully relaxed, visible as reduced pop-ins in the annealed and centre region of the larger diameter sample loading curves of $Pd_{77.5}Si_{16.5}Cu_6$ and $Zr_{65}Cu_{15}Al_{10}Ni_{10}$ in Fig. 3. G^* determined here is on a larger structural scale than that proposed for G^* [4] and G_c [5], though, by using nanoindentation it is possible to obtain an indication of local values that are not sample averages, and reflects a higher degree of resolution as a result of the intrinsic nature of the nanoindentation test itself. This continuous structural variation means that under certain circumstances BMG rods should be considered a composite of differing local structures, and so do not possess a single G, B and E; moduli determined by techniques such as sound wave velocities are a global average.

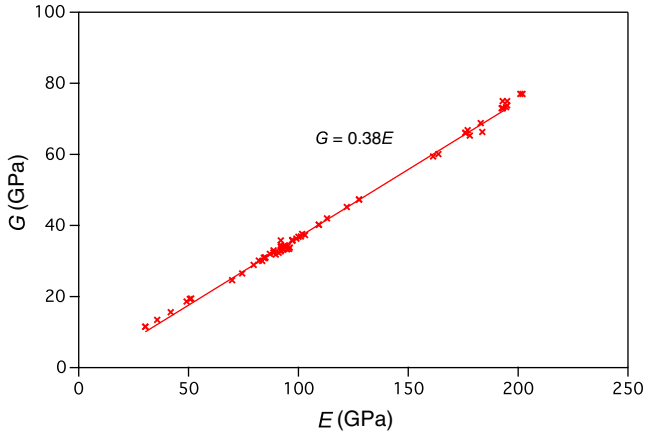

Fig. 5. Plot of G versus E for the BMGs in Table 1 of [1,19].

Table 3
Comparison of magnitude of change in G^* across all as-cast diameters (G^*_{min}/G^*_{max}) and due to surface effects in the 1 mm rods of each alloy.

	$\left(\frac{G^*_{min}}{G^*_{max}}\right)$	$\left(\frac{G^*_{edge}}{G^*_{centre}}\right)_{1mm}$
$Pd_{77.5}Si_{16.5}Cu_6$	0.60	0.87
$Zr_{65}Cu_{15}Al_{10}Ni_{10}$	0.61	0.77
$Ce_{70}Al_{10}Ni_{10}Cu_{10}$	0.94	0.94

The plastic zone size, r_p, of a material represents the plastic region generated ahead of a crack tip when the applied stress exceeds the yield point, σ_y, of the material. It can be considered the length scale over which stable shear banding is possible in BMGs [21]. In the case of plane stress, where K_{1C} is fracture toughness:

$$r_p = \frac{K_{1C}^2}{2\pi\sigma_y^2} \tag{4}$$

Then, as shear yield stress, $\tau_y = \sigma_y/2$ and $G = \tau_y/\gamma_c$, where γ_c is the critical shear strain for BMGs (0.0267) [1], the following relationship relates r_p to G:

$$r_p = \frac{K_{1C}^2}{8\pi G^2\gamma_c^2} \tag{5}$$

As with G^*, pronounced variation in r_p is expected as a result of its inverse dependence on G^2; this illustrates the structural diversity, and therefore range of mechanical response, that is possible from a single alloy (global softening) and within a cast rod (surface softening). The analysis presented here, with regard to variation in G^* and r_p, demonstrates the structural sensitivity of BMGs to thermal history (i.e. cooling conditions). Replication of mechanical data between researchers is therefore problematic due to variations in experimental technique and intrinsic cooling conditions of the casting arrangement resulting in different structures. As more structural states may be present in fragile glass formers (see Fig. 4) it may be these alloys that are most sensitive to their preparation route and might exhibit the largest range in plastic response.

Reported in [22] is that shot-peening induced residual compressive surface stresses and a soft surface in a Ti-based BMG, resulting in an $H_{v(edge)}/H_{v(centre)}$ value of 0.88. Plasticity increased to an average of 11% (and a maximum of 22%) from an average of 6% in the non-peened state. A soft surface may have benefitted this, due to a reduced energy barrier to STZ activation in the surface region, as is shown in Fig. 3, which could enhance macroscopic plasticity. The results of the present study show $H_{v(edge)}/H_{v(centre)}$ for 1 mm $Pd_{77.5}Si_{16.5}Cu_6$ and $Zr_{65}Cu_{15}Al_{10}Ni_{10}$ are 0.94 and 0.78 (see Fig. 2a and b) respectively and so are in broad agreement with the observations made for the shot-peened sample, though it must be considered that the extent of work softening may not be consistent at each site, as previously mentioned. Surface softening in as-cast components might then have an effect on macroscopic plasticity.

5. Conclusion

$Pd_{77.5}Si_{16.5}Cu_6$, $Zr_{65}Cu_{15}Al_{10}Ni_{10}$ and $Ce_{70}Al_{10}Cu_{10}Ni_{10}$ BMGs, with a range of fragility indexes and mechanical performance, were selected to perform nanoindentation along traverses from the edge of both as-cast and annealed rods towards their centre, generating hardness and reduced modulus profiles for the glasses as a function of rod diameter. Surface softening is not found to be a universal phenomenon in copper-mould cast BMGs, as its magnitude continuously decreases with increasing diameter resulting in its absence in rods beyond a critical size. This is attributed to longer *in-situ* annealing times at higher temperatures in large diameter samples activating more atomic relaxation events. Enhanced diversity in the potential energy landscape of fragile glasses may permit a large range of different atomic sites, enabling a range of local co-ordinations to be present at room temperature, and so fragile glasses may be the most likely to show the surface softening effect.

Samples that surface soften contain different local structures at the centre and edge, each with differing tendencies for STZ nucleation, resulting from reduced atomic connectivity and a resulting decrease in G. A measure of the shear modulus, G^*, is extracted for each indent location, and a range of values is found across a single rod, illustrated by a 33% difference between the centre and edge of 1 mm $Zr_{65}Cu_{15}Al_{10}Ni_{10}$. This causes increased shear band nucleation, identifiable as more pop-ins in the loading curves at the edge of 1 mm rods in comparison to the more relaxed larger diameter and annealed structural states and may result from more energetic energy minima at these sites in the energy landscape. The range in G^* and r_p reflects the varied mechanical performance that is possible within a single alloy system, and the potential sensitivity of mechanical performance to preparation history.

Acknowledgements

Technical assistance provided by D. Bussey and P. Hawksworth is acknowledged. Funding for this work was provided by the Innovative Metals Processing Centre (IMPC) and through a studentship for JDP from the Engineering and Physical Sciences Research Council (EPSRC).

References

[1] W.L. Johnson, K. Samwer, Phys. Rev. Lett. 95 (2005) 195501.
[2] M. Jiang, L. Dai, Phys. Rev. B 76 (2007) 5.
[3] S. Pauly, M.H. Lee, D.H. Kim, K.B. Kim, D.J. Sordelet, J. Eckert, J. Appl. Phys. 106 (2009) 103518.
[4] S.J. Poon, A. Zhu, G.J. Shiflet, Appl. Phys. Lett. 92 (2008) 261902.
[5] Y.Q. Cheng, A.J. Cao, E. Ma, Acta Mat. 57 (2009) 3253.
[6] Y. Liu, H. Bei, C.T. Liu, E.P. George, Appl. Phys. Lett. 90 (2007) 71909.
[7] C.A. Schuh, T.G. Nieh, Acta Mat. 51 (2003) 87.
[8] C.A. Schuh, A.C. Lund, T.G. Nieh, Acta Mat. 52 (2004) 5879.
[9] J.D. Plummer, I.A. Figueroa, R.J. Hand, H.A. Davies, I. Todd, J. Non-Cryst. Solids 355 (2009) 335.
[10] Y. Liu, H. Wu, C.T. Liu, Z. Zhang, V. Keppens, Appl. Phys. Lett. 93 (2008) 151915.
[11] G.V. Raynor, Metallurgical Thermochemistry, vol. 5, Pergammon Press, 1979.
[12] I.A. Figueroa, H.A. Davies, I. Todd, Phil. Mag. 89 (2009) 27.
[13] W.C. Oliver, G.M. Pharr, J. Mater. Res. 7 (1992) 6.
[14] H. Bei, S. Xei, E.P. George, Phys. Rev. Lett. 96 (2006) 105503.
[15] C.A. Angell, Science 267 (1995) 1924.
[16] R.J. Speedy, J. Phys. Chem. B 103 (1999) 4060.
[17] P.G. Debenedetti, F.H. Stillinger, Nature 410 (2001) 259.
[18] M. Miller, P. Liaw, Bulk Metallic Glass, Springer, 2008, p. 41.
[19] J.J. Lewandowski, W.H. Wang, A.L. Greer, Phil. Mag. Lett. 85 (2005) 77.
[20] H.M. Ledbetter, Mater. Sci. Eng. 27 (1977) 133.
[21] D.C. Hoffmann, J.Y. Suh, A. Wiest, G. Duan, M.L. Lind, M.D. Demetriou, W.L. Johnson, Nature 451 (2008).
[22] Y. Zhang, W.H. Wang, A.L. Greer, Nat. Lett. 5 (2006) 857.